Applied Energy 121 (2014) 149–158

Contents lists available at ScienceDirect

Applied Energy

journal homepage: www.elsevier.com/locate/apenergy

A feasibility study of a stand-alone hybrid solar–wind–battery system for a remote island

Tao Ma *, Hongxing Yang, Lin Lu

Renewable Energy Research Group (RERG), Department of Building Services Engineering, The Hong Kong Polytechnic University, Hong Kong

HIGHLIGHTS

- A feasibility study of a hybrid solar–wind–battery system is carried out.
- Techno-economic evaluation is conducted for this proposed system.
- Thousands of cases are simulated to achieve an optimal system configuration.
- The performance of the proposed system is analyzed in detail.
- A sensitivity analysis on its load and renewable energy resource is performed.

ARTICLE INFO

Article history:
Received 19 November 2013
Received in revised form 18 January 2014
Accepted 25 January 2014
Available online 28 February 2014

Keywords:
Solar–wind–battery system
Techno-economic evaluation
Net present cost (NPC)
Standalone renewable energy system
Cost of energy (COE)

ABSTRACT

This paper presents a detailed feasibility study and techno-economic evaluation of a standalone hybrid solar–wind system with battery energy storage for a remote island. The solar radiation and wind data on this island in 2009 was recorded for this study. The HOMER software was employed to do the simulations and perform the techno-economic evaluation. Thousands of cases have been carried out to achieve an optimal autonomous system configuration, in terms of system net present cost (NPC) and cost of energy (COE). A detailed analysis, description and expected performance of the proposed system were presented. Moreover, the effects of the PV panel sizing, wind turbine sizing and battery bank capacity on the system's reliability and economic performance were examined. Finally, a sensitivity analysis on its load consumption and renewable energy resource was performed to evaluate the robustness of economic analysis and identify which variable has the greatest impact on the results. The results demonstrate the techno-economic feasibility of implementing the solar–wind–battery system to supply power to this island.

1. Introduction

Energy is an essential requirement for all social activities, production of all goods and the provision of all services [1]. On the other hand, energy is also and still to be the biggest crisis to human beings, since currently the majority of the energy used on earth comes from conventional fossil fuels, and some of them will be exhausted in several decades according to the recent exploring and consuming rate. Moreover, there are still about 1.5 billion inhabitants worldwide still having no access to electricity [2,3]. The energy supply for those remote islands and villages is commonly powered by diesel generators. However, they felt more and more stressed since they often face exaggerated fuel costs due to significant rise in diesel price and extra costs of shipment. Additionally, the negative environmental effects from the employment of diesel damage the local ecological system and cause noise, water, soil and air pollution [4]. In the issue, they suffer from energy shortage or blackouts frequently.

Fortunately, remote areas are usually rich of locally available renewable energy resources. Due to the rising cost of diesel fuel and the rapidly declining cost of renewable energy technologies, the energy supply by renewables is now becoming competitive with conventional energy, thus encouraging widely utilization of renewable energy systems (RESs) for off-grid power supply, such as PV–battery, wind–battery, PV or wind based pumped storage, or hybrid systems [5–11]. Up to now, research on RESs is usually carried out in the field of system modeling, simulation, component sizing, economic analysis, and particularly system optimization [12–17]. To carry out such research, the simulation models and computer tools are generally required. Totally 37 computer tools for analyzing the RESs has been reviewed in [18], and a review of

* Corresponding author. Tel.: +852 2766 5863; fax: +852 2765 7198.
E-mail address: tao.ma@connect.polyu.hk (T. Ma).

http://dx.doi.org/10.1016/j.apenergy.2014.01.090
0306-2619/

methodology of optimizing the hybrid RES was carried out in [19]. Among the simulation tools, HOMER (Hybrid Optimization Model for Electric Renewable) software is one of the most widely used for standalone RESs [12]. This software can assist in the design of micropower systems and facilitate the comparison of power generation technologies across a wide range of applications [20]. Using HOMER for RES modeling, simulation and techno-economic analysis has been the subject matter of substantial earlier studies, for example, the possibility of achieving energy autonomy in an island using PV, wind turbine, battery and biogas generator was examined in [21]; the pre-feasibility study of a stand-alone power generation using hybrid renewable energy with hydrogen energy storage was conducted in [22], a small Hydro/PV/Wind hybrid system in Ethiopia was examined in [23], and the economic performance of hybrid photovoltaic–diesel–battery power systems for residential loads in hot regions was analyzed in [24].

The present study is based on a research project on power supply for a small remote island in Hong Kong. The operation performance of the 19.8 kW p PV system in Stage 1 has been evaluated by the research group [25]. In Stage 2 of the island redevelopment, the wind turbine will be introduced and system capacity will increase to improve the living and facilities conditions for residents on the island. The paper focuses on investigating the feasibility of utilizing solar and wind energy to meet the electricity requirements of this remote island in conjunction with the battery storage. Specially, some basic research works in this study are reported, including feasibility study, system design, and techno-economic evaluation. The solar radiation, wind speed and ambient temperature data in 2009 has been recorded on that island for this study, and then renewable energy resource and the merit of hybrid solar and wind system have been evaluated. HOMER software is employed as a platform for sizing and optimizing the proposed system. To achieve an optimal autonomous system configuration for this island, thousands of cases in hourly basis are carried out and compared with regards to system net present cost (NPC) and cost of energy (COE). Emphasis has also been placed on analyzing the expected performance of the proposed system in detail. Moreover, the effects of the PV, wind turbine, battery bank capacity on the system's reliability and economic performance were examined. Finally, sensitivity analysis on load and renewable energy resource is performed to evaluate the robustness of economic analysis and identify which variable has the greatest impact on the results.

2. System description

There are ongoing attempts to accomplish the hybrid solar and wind system employing a battery bank. The hybrid solar–wind power generation systems can effectively improve the system energy usage factor, advance energy supply reliability, and reduce the energy storage requirements, due to complementary nature of solar energy and wind energy supply. Substantial research [9,14,26–29] has been conducted on this area, demonstrating that the hybrid system with energy storage is techno-economically viable for rural electrification in remote areas.

2.1. System configuration

The system architecture and energy flow for the proposed hybrid solar–wind system with battery storage is shown in Fig. 1. The system mainly consists of PV array, wind turbine (WT), battery bank, inverter (aka converter), controller, and other accessory devices and distribution cables. The DC power output from the PV array and WT is converted into AC by the inverter to directly supply the base load, while available excess energy is fed into the battery bank. When the battery bank is fully charged, the surplus energy is dumped if there is no more energy demand. The battery bank releases power to the load when the renewable energy output is unavailable or is insufficient to supply the load. The main power distribution component is the inverter, to which the AC and DC buses are connected. The PV array, WT and batteries supply the DC bus, and the AC bus carries power to the load side (assuming that all loads utilize AC).

2.2. System control

The system can be easily controlled because there is only one dispatchable power source, i.e. the battery bank. Whenever the net load, i.e. the difference between the actual load and the renewable energy output, is negative, meaning that power supplied by

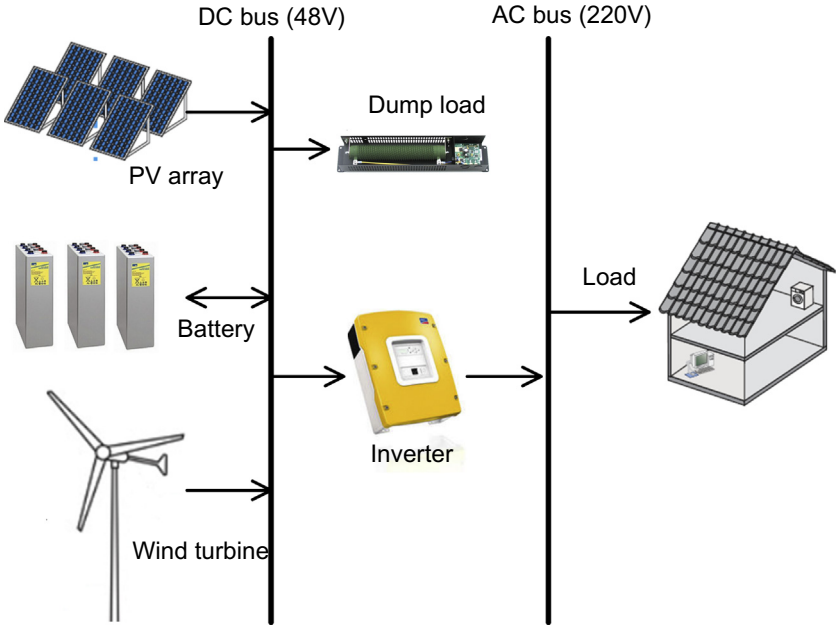

Fig. 1. The energy flow diagram of the proposed hybrid solar–wind system with battery storage.

the renewables is sufficient to serve the load, the excess energy is then used to charge the battery bank and any further surpluses dumped. Whenever the net load is positive, the only supplementary power source battery bank releases energy to satisfy the load. The operation strategy of this kind system is shown in Fig. 2.

3. System modeling

3.1. Island load profile

In this study, the daily base load on this island was estimated at 250 kW h/day, and then was synthesized by adding some randomness for different days and months, to create a quite reasonable profile for this island in a year. The hourly load profile during different months is illustrated in Fig. 3.

3.2. Renewable energy resource

The meteorological data on this island was collected by Hong Kong Observatory in 2009, including solar radiation, wind speed and ambient temperature. Fig. 4a presents the average solar and wind energy resources by month. The inherent complementary nature is displayed, the summer provides a relative good solar energy resource but poor wind condition, while the winter has a crosscurrent. Additionally, Fig. 4b demonstrates the hourly and daily complementary characteristic that the wind often blows when the sun does not shine and vice versa. The figures show that solar and wind energy together can provide greater value than either one alone and a better utilization factor for the available energy, and thus less energy storage capacity is needed.

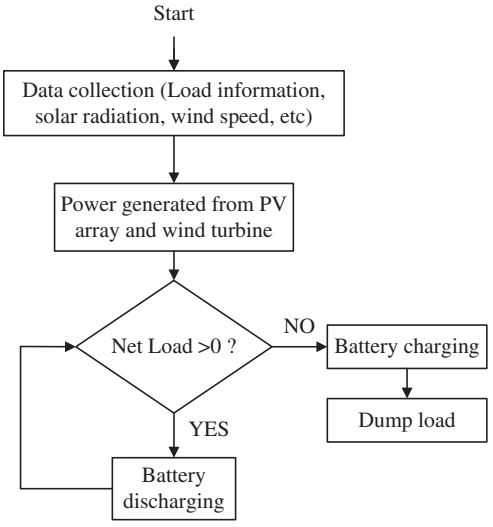

Fig. 2. Operating strategy of this hybrid solar and wind system employing a battery bank.

3.3. System components information

3.3.1. PV modules

The PV module (model: STP210-18/Ud) from Suntech was employed in the study. The basic information of the selected PV module is summarized in Table 1. The rated power of the module is 210 W and the efficiency of the module in stand test condition (STC) is 14.3%.

In this study, the initial capital cost of a PV module was assumed as $ 2.0/Wp on the basis of rapid decrease trend of PV module price (including the PV module and array installation costs). The replacement cost was considered to be the same as the initial cost. The operating and maintenance (O&M) cost was assumed to be zero since it is negligibly small [30].

The energy output of the PV generator (kW h) was calculated based on the following equation:

$$P_{PV} = f_{PV} \cdot Y_{PV} \cdot \frac{I_T}{I_S} \quad (1)$$

where Y_{PV} is the rated capacity of the PV array (kW); I_T the global solar radiation incident on the surface of the PV array (kW h/m^2); and I_S is 1000 W/m^2; f_{PV} is the PV derating factor, which accounts for the negative effects of dust, wire losses, elevated temperature, or anything else on the performance of PV panel. A derating factor of 80% was employed in this study [20].

3.3.2. Wind turbine

The wind turbine Proven 11 (known as KW6) was assumed to be installed. The details for this wind turbine are presented in Table 2, in which the cost information for this wind turbine was provided by the dealer.

Based on the power curve from the manufacturer (Fig. 5), the power output from the wind turbine can be modeled as:

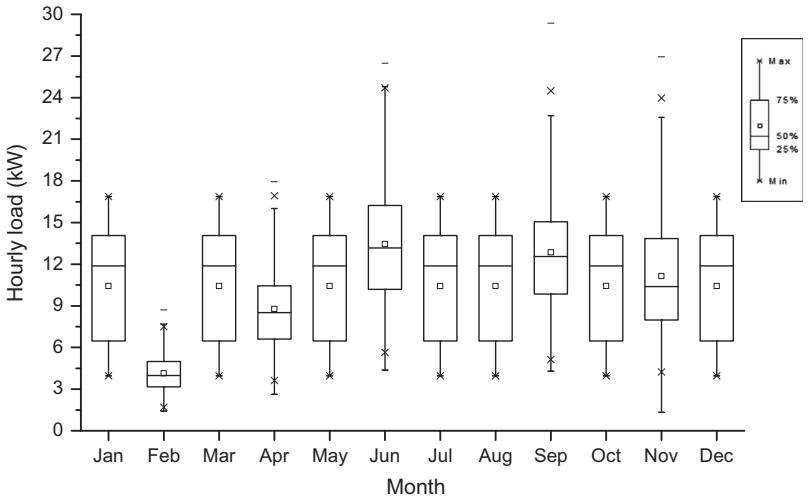

Fig. 3. Hourly load during a year on this island.

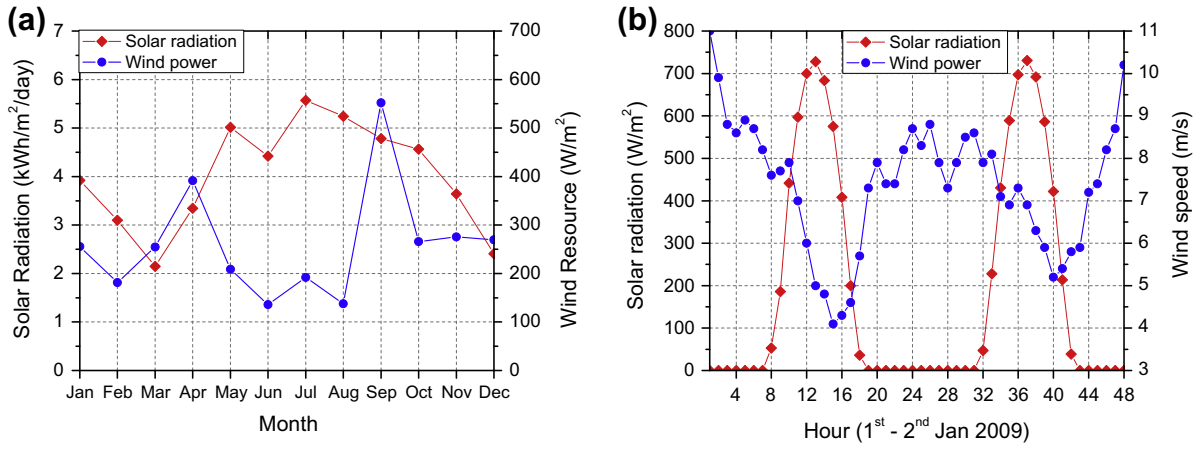

Fig. 4. The solar and wind energy resource on the island (a) monthly energy density in 2009 and (b) daily solar radiation and wind speed distribution on 1st-2nd January 2009.

Table 1
Details of PV module.

PV	
Manufactory	Suntech
Model	STP210-18/Ud, Polycrystalline
Maximum power at STC (Pmax)	210 W
Optimum operating voltage (Vmp)	26.4 V DC
Optimum operating current (Imp)	7.95 A
Dimensions	1482 × 992 × 35 mm
No. of solar cells (156 × 156 mm)	54 (6 × 9)
Capital cost	$ 2000/kWp
Replacement cost	$ 2000/kWp
Operating and maintenance cost	$ 0/Wp
Derating factor	80%
Slope (degree)	22.3
Lifetime	25 years
Search space of PV capacity	0, 50–250 kW (with an interval of 5 kW)

Table 2
Details of wind turbine.

Wind Turbine	
Manufactory	Proven/Kingspan Renewables Ltd.
Model	Proven 11 (KW6)
Rated power	5.2 kW (1 min average at 11 m/s)
Peak power	6.1 kW
Reference annual energy	8949 kW h (5 m/s, 10 m hub)
Output voltage available	48V DC/300 V DC
Cut in speed	3.5 m/s
Cut out speed	N/A (Continuous operation)
Survival wind speed	Designed to Class 1 (70 m/s)
Hub/tower heights	9 m/11.6 m/15m/20 m
Capital cost per unit	$ 27,658 (£ 20,912)
Replacement cost per unit	$ 27,658 (£ 20,912)
Operating and maintenance cost per unit	$ 500/year
Lifetime	20 years
Search space of WT number	0–12 units (with an interval of 1)

The underline in table is used to indicate the parameters selected in this study.

$$P(v) = 5.5 \times e^{\left(\frac{v-13.8}{4.6}\right)^2} + 2.2 \times e^{\left(\frac{v-9.15}{3.5}\right)^2} \quad (2)$$

3.3.3. Battery bank

The deep cycle battery is widely used in off-grid renewable energy systems. The datasheet for the battery from Hoppecke already exists in the simulation software, as shown in Table 3.

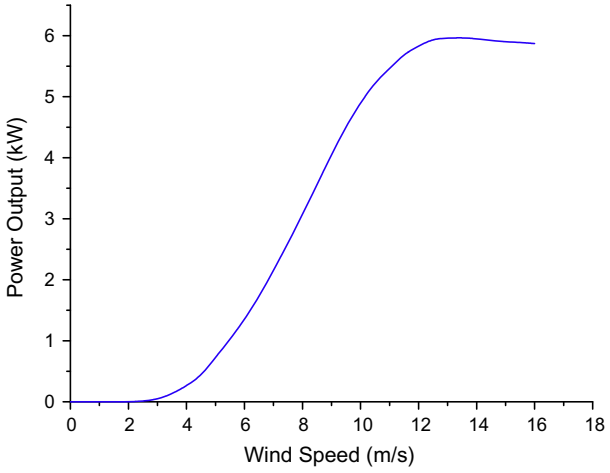

Fig. 5. Power curve of the wind turbine.

Table 3
Details of the selected battery.

Manufactory	Hoppecke
Nominal capacity	3000 Ah
Nominal voltage	2 V
Roundtrip efficiency	86%
Maximum depth of discharge	70%
Lifetime throughput	10,196 kW h
Capital cost per unit	$1644 (RMB 10,383)
Operating and maintenance cost per unit	$10/year
Search space in HOMER	0–480 units (with an interval of 24)

The sizing approach to coarsely determine the required number of batteries is shown in Eqs. (3)–(5).

$$C_{Ah} = \frac{E_c}{\eta_B \cdot DOD \cdot V_B} = \frac{n_{day} \cdot E_{load}}{\eta_B \cdot DOD \cdot V_B} \quad (3)$$

$$n_{battry} = \frac{C_{Ah}}{C_{single}} \quad (4)$$

$$n_{string} = \frac{n_{battery}}{48/V_B} \quad (5)$$

where n_{day} is the number of autonomous days powered solely by the battery storage bank; E_{load} is the daily energy consumption

(250 kW h); $E_c = n_{day} \cdot E_{load}$ is the summary of energy demand for the continuous number of autonomous days (if 5 days of autonomy is assumed, the system power supply availability can be larger than 95%, according to practice from the handbook [31]); η_B is the overall battery and inverter efficiency; V_B is the battery rated voltage; *DOD* is the allowable depth of discharge; C_{single} is the storage capacity of a single battery; $n_{battery}$ is the total number of batteries; and n_{string} is the string number. The sum of the voltages provided by each string should equal the nominal system voltage of the DC bus (48 V), meaning that each string consists of 24 batteries only.

The kinetic battery model [32,33] was assumed in this study to find the maximum allowable charging and discharging rates. This model treats the battery as a "two tank" system. One tank (part of the battery's energy storage capacity) provides immediately available energy while the second is chemically bound which can only be charged or discharged at a limited rate. In addition, an optional control parameter called the set-point state of charge (SOC) was applied in this study. When a set-point SOC is applied, the renewable energy will continue charging the battery bank until it reaches the specified SOC. Otherwise, the battery bank will start discharging as soon as it can supply the load. The set-point SOC helps avoiding situations where the battery experiences shallow charge–discharge cycles close to its minimum SOC. In real systems, such situations are harmful to battery life. In this study, the battery set-point SOC was set at 80%, which is also recommended by Lambert and Lilienthal [33]. Based on the cycles-to-failure curve in Fig. 6, the lifetime throughput, the amount of energy that can cycle through the battery before failure, can be calculated using the following equation:

$$Q = f \cdot d \cdot \frac{q_{\max} V_B}{1000} \tag{6}$$

where Q is the lifetime throughput of a single battery (kW h), f is the number of cycles to failure, d the depth of discharge (%), $q_{\max}$ is the maximum capacity of the battery (Ah) and V_B is the nominal voltage of the battery (V).

4. Results and discussion

4.1. System physical configuration

Based on the meteorological data and load consumption, thousands of cases were carried out to achieve an optimal system configuration, which is shown Fig. 7. The simulation results from HOMER show that the optimal system comprises PV array (145 kW), WT (2 units, 10.4 kW), battery bank (144 units, 6 stings, totally 706 kW h) and converter (6 units, 30 kW). The performance of this optimal system is discussed in Sections 4.2–4.5, and a sensitivity analysis on the key parameters is then conducted to identify their impact on the results.

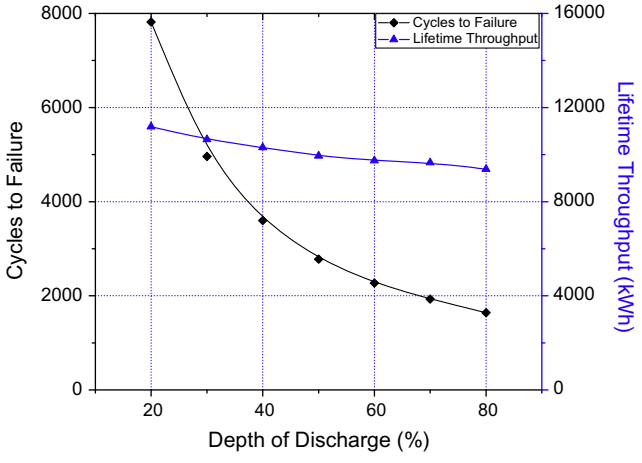

Fig. 6. Lifetime cycles-to-failure and throughput of the battery.

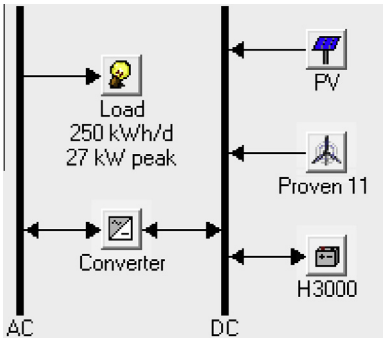

Fig. 7. System physical configuration of the proposed hybrid solar and wind system with battery storage in HOMER.

4.2. Operating performance of system components

A summary of operating performance and some economic results of PV, wind turbine and battery bank is presented in Table 4. It can be seen that the capacity factors of PV array and WT were relatively low because of large amounts of wasted energy. The levelized costs for the PV and WT were \$0.128 and \$0.2 per kW h, respectively. The energy cost for the battery bank was zero because the only charging source is the excess energy from PV and WT. However, the battery wear cost of \$0.174/kW h was significantly high, accounting for approximately 30% of the COE. The battery cost was even higher than that of the PV module, which could explain in some cases why the end-users might cut down or discard the energy storage devices and introduce more renewable energy generators. Such approach, however, may result in a substantial waste of energy.

The monthly mean electric production from PV array and WTs is presented in Fig. 8. It can be noted that solar production predominated, providing almost 86% of the total production during the simulation year. The PV output was extremely high in the summer months from July to October. This is a favorable characteristic since electricity demand is strong in the summer due to high cooling load. In contrast, the wind energy contribution was found to be significant in April and September but less in other months.

The simulation results for the battery bank state of charge (SOC) are presented in Fig. 9. SOC values between 90% and 100% existed for approximately 74% of the time, and more than 90% of the time witnessed the SOC vales higher than 80%, indicating that the battery bank was only used in "shallow" fashion for most of the time. The result also illustrates the hourly battery bank SOC profile during the simulation year. It can be seen that most of the time the SOC was relatively high. In only two months did high depth of discharge occur: the lowest SOC values were in March and August at 35% and 30%, but averaging 65% and 76%. This phenomenon is explained by relatively poor renewable resources availability in March and a high cooling load in August. Thus there must be sufficient capacity of the battery to supplement supplies in those two months from the stored energy, ensuring a sustainable and continuous power supply. On the other hand, it can be seen that the battery bank size could be greatly reduced if some load is allowed

Table 4
Components operating performances of solar–wind–battery during the simulated year.

Parameters	Data	Units	Parameters	Data	Units
1. PV			**3. Battery**		
Rated capacity	145	kW	Batteries number	144	
Mean output	20	kW	Strings in parallel	6	
Capacity factor	14	%	Usable nominal capacity	605	kW h
Total production	177,882	kW h/yr	Autonomy	58.1	h
Hours of operation	4392	h/yr	Lifetime throughput	1,468,224	kW h
Levelized cost	0.128	$/kW h	Energy in	37,829	kW h/yr
2. Wind			Energy out	32,561	kW h/yr
Total rated capacity	10.4	kW	Battery wear cost	0.174	$/kW h
Mean output	3.4	kW	Expected life	20	year
Capacity factor	32.5	%			
Hours of operation	7688	h/yr			
Total production	29,584	kW h/yr			
Levelized cost	0.2	$/kW h			

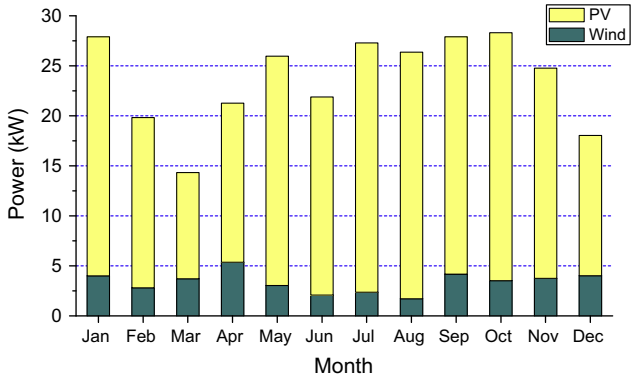

Fig. 8. Daily mean powered generated by PV and wind in different months.

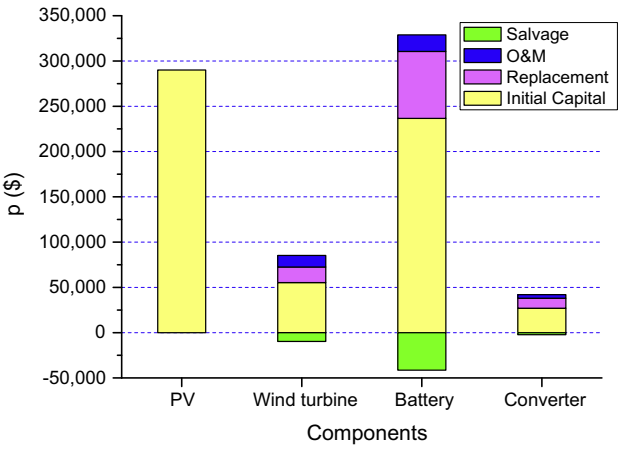

Fig. 10. Cash flow break-down by components and cost type.

not to be met under conditions of extreme unsuitable weather and extreme peak load.

4.3. Total cost break-down

The cash flow break-down by components and cost type is shown in Fig. 10. The money appeared in this study are US dollar ($). The initial cost (IC) and total net present cost (NPC) of the above system were found to be $608,932 and $693,114, respectively. The corresponding levelized cost of energy (COE) was $0.595/kW h, approximately three time of the current electrical tariff in Hong Kong [34,35]. However, this is still considered as a cost-effective solution in comparison the diesel generator or grid extension by submarine cables and overhead lines.

It should be noted that the cost of the battery bank is nearly 50% of the total NPC, of which the IC occupies about 82%. This indicates that the cost of a storage subsystem in a stand-alone hybrid renewable system to be dominant. The cost of a 145 kW PV array, IC only, accounts for 36% of the system total NPC, followed by the WT cost, which takes up approximately 10%, including the O&M and replacement costs. The least cost item is the converter, at 5% of the total NPC.

4.4. Energy flow or energy balance analysis

Fig. 11 summarizes the energy flow of the whole system. 84% of the renewable energy output was contributed by the PV array and 16% by WTs. However, almost 48.6% of the total output was excess to requirements and had to be transferred to the dump load as spilled energy [36]. It should be mentioned that this excess renewable energy to un-used results from lack of demand or storage capacity. Among the total useful electricity (106,583 kW h), 85.6% was consumed by the end-users, 4.9% was used to cater for battery bank losses and 9.5% for converter losses.

4.5. Hourly simulation results

An example of the hourly simulation results during four consecutive days is illustrated in Fig. 12. In such a system, the battery

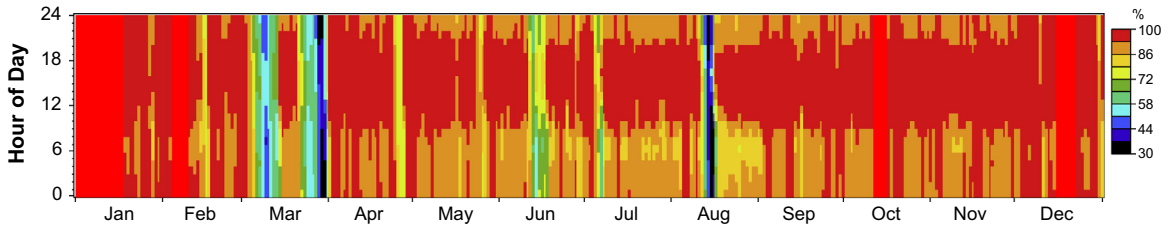

Fig. 9. Rainbow profile of battery bank state of charge during the simulated year.

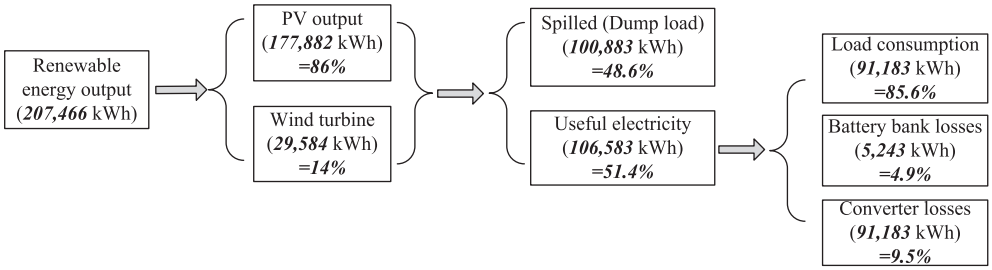

Fig. 11. Summary of the energy flow during the simulated year.

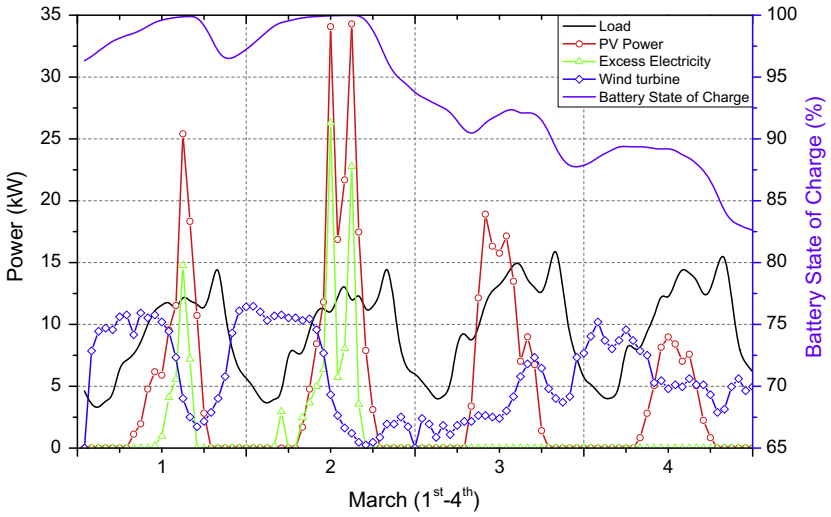

Fig. 12. Hourly sample simulation results for four consecutive days (1st to 4th March).

bank absorbs energy when the renewable energy output exceeds the load, and discharges energy when the load exceeds the renewable output.

The red line of the hollow circles and the blue line of the hollow diamonds display the PV output and WT output. Usually the wind energy resource was excessive late at night and during the early morning hours. Surplus solar energy was typically available during the middle of the day. The black line illustrates the load profile for this island. After serving the load, the excess electricity was used to charge the battery bank. The top violet colored line illustrates the battery state of charge (SOC) and indicates the amount of energy stored in the battery bank. If the excess electricity was more than enough to fully charge the battery bank, the surplus was then fed into the dump load, represented by the green line of hollow triangles.

During 1st and 2nd March, the solar and wind resources were good and able to cater for the demand. Thus excessive power was produced in the afternoon. It was noticed that for some hours the surplus energy was not fully transferred to the battery bank even though its SOC had not reached a 100% level. This is because it is limited by the maximum allowable charging rate and current of the selected battery, and it is also dependent on the recent charging and discharging history of the batteries, which is the basic principle of the kinetic battery model [32].

The battery bank was periodically charged or discharged during the first two days, while the SOC values dropped during the third and fourth day due to poor solar radiation. It is found that the lowest value of 82% occurred on the fourth day, but still much higher than the allowable minimum SOC.

During the whole simulation period, depletion of the battery energy might occasionally occur when the renewable source output is not able to meet the demand, indicating the existence of some energy shortfalls, recorded as 'unmet load'. Although the maximum annual capacity shortage was set at 0% in this study, an extremely small unmet load, amounting to approximately 66.6 kW h (0.07% of the total load) was experienced during the simulated year.

4.6. The effects of the PV, wind turbine, battery bank capacity on simulation result

The effect of variation in PV capacity and battery number on the total NPC is demonstrated in Fig. 13. In this case, the WT and converter were fixed at 2 units and 30 kW, respectively. The results show that the optimal system type (OST) appears at 145 kW PV with 6 battery strings. The results indicate that an increase in PV capacity can reduce the battery bank size. But only the optimal system configuration chosen in the study has the lowest NPC.

Fig. 14 demonstrates how PV capacity, number of battery strings, total NPC, and excess electricity produced vary with the number of WTs. It can be seen that if no WTs are installed, the PV-only energy supply system has an extremely high PV capacity (240 kW) with 6 strings of batteries. The NPC value is about $855 k (COE: $0.734) and 63% of total electrical production is dumped, making this system very expensive. The system with two WTs is considered to be the OST because it possesses the lowest NPC, COE and excess electricity, and the PV size in OST obviously decreases markedly to 145 kW. As increasing numbers of WTs are introduced, the battery bank and PV capacities can be reduced but the NPC, COE, excess electricity and wind energy contribution rise.

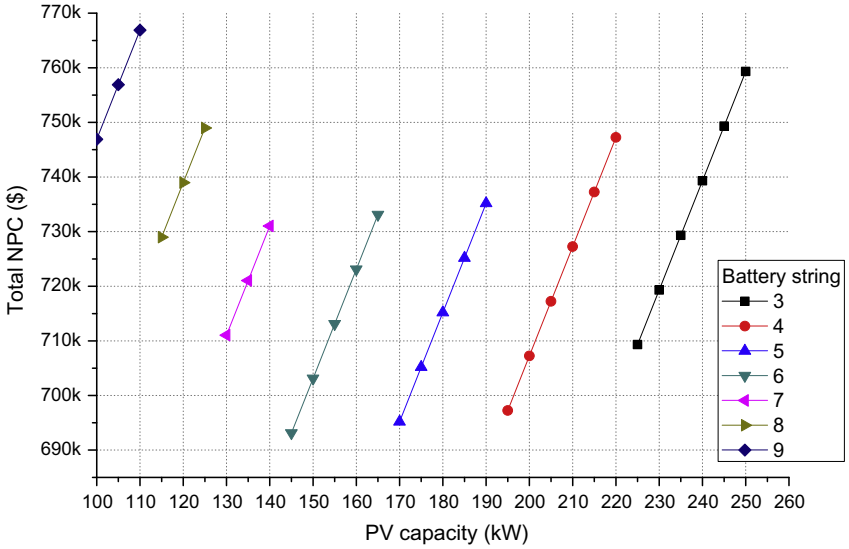

Fig. 13. The effect of PV capacity and battery string number on total NPC.

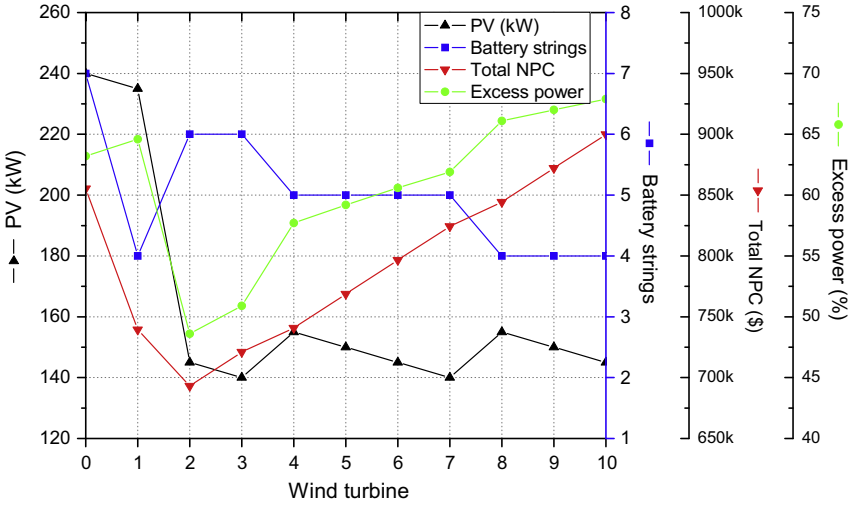

Fig. 14. PV, battery, NPV and excess power versus WT number.

Table 5
The optimal system configuration under different average daily load from 150 to 400 kW h/day.

Mean daily load (kW h)	System type	PV size (kW)	WT number	Battery strings	Converter (kW)	Total NPC ($)	COE ($/kW h)	Excess electricity (%)
150	PV/Wind/Battery	130	1	2	20	420,266	0.601	63.3
	PV/Battery	150	–	4	20	518,289	0.741	64.7
200	PV/Wind/Battery	110	2	5	25	568,542	0.61	48.3
	PV/Battery	205	–	5	25	682,861	0.732	65.6
250	PV/Wind/Battery	145	2	6	30	693,114	0.595	48.6
	PV/Battery	240	–	7	30	855,365	0.734	63.2
300	PV/Wind/Battery	235	2	5	35	831,823	0.595	59.7
	PV/Battery	320	–	7	35	1,022,006	0.731	66.9
350	PV/Wind/Battery	210	3	8	40	970,099	0.595	50.6
	PV/Battery	355	–	9	40	1,194,510	0.732	65.2
400	PV/Wind/Battery	245	3	9	50	1,101,312	0.591	50.8
	PV/Battery	390	–	11	45	1,367,014	0.733	63.8

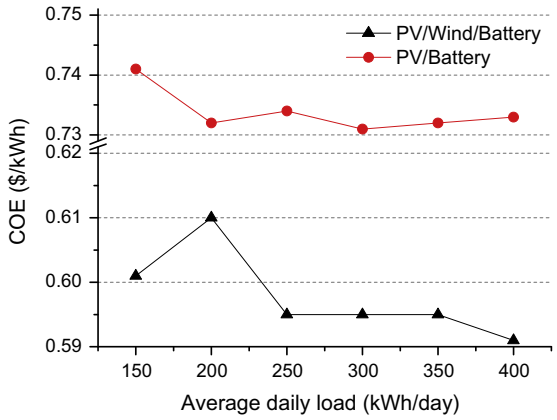

Fig. 15. Cost of energy ($/kW h) for different system types against energy demand.

4.7. Sensitivity analysis on load consumption and renewable energy resource

4.7.1. The effect of the load demand

As mentioned above, the daily load consumption in the base case was assumed as 250 kW h. To leave some margin for the island, load consumptions varying from 150 to 400 kW h/day were investigated.

The optimal system configurations under different load levels are displayed in Table 5. As load increases, the PV capacity, WT number, battery number, and converter size all increase gradually. The COE of solar–wind–battery and solar–battery system are in the ranges of $0.59–$0.61 and $0.73–$0.75 (as shown in Fig. 15).

Compared with the PV-only system, the hybrid solar–wind system produces less waste electricity, lower storage capacity and lower COE values under different load levels, indicating that the complementary characteristic of wind and solar energy resources can help to reduce the generation and storage capacity. In addition, the economic benefits of solar–wind–battery system become more significant the greater is the consumption load.

4.7.2. The effect of renewable energy sources (solar radiation and wind speed)

The effects of available solar and wind energy potential on the system type, system configuration and cost are examined. The optimal system type graph under various solar radiation intensities and wind speeds is presented in Fig. 16. If the average wind speed is lower than 3.5 m/s, the PV–battery systems provide the lowest COE, because the WT cannot start or else outputs little energy at such low wind speeds. For the average wind speed between 3.5 and 4 m/s, PV–wind–battery systems are cost effective for low solar radiation values and PV–battery systems for high solar radiation values. When the average wind speed is 4 m/s, it seems that introducing one or two WTs could be economical since it begins to produce electricity.

5. Conclusions

The study shows that the island's existing diesel generator could be fully replaced by a 100% renewable energy power generation system. The combination of solar energy, wind energy and battery storage can supply continuous power to this island. The optimal system mainly comprises 145 kW PV array, 2 WTs, 168 batteries and a 30 kW converter. The result illustrates that 84% of the load was covered by the PV array and 16% by WTs. However, the dumped energy was as high as 100,883 kW h, about 48.6% of the total production, due to timing mismatch between power demand and generation. If a small percentage capacity shortage or some degreed of unmet peak load is allowed, the sizes of the system components could be greatly reduced and the system's economic performance could be enhanced.

The results also demonstrate that the proposed hybrid solar and wind power system with battery storage is a practical and cost-effective solution for this remote island. The levelized cost of energy (COE) of this system is $0.595/kW h. With expected continuing rapid development in renewable energy industry and upgrades in storage technology, the system's cost will be reduced and hence off-grid RESs sited in remote places could be more promising. It can be expected that in the near future the transition from diesel to high renewable energy penetration will be increasingly popular in remote areas for power generation.

Acknowledgments

The work described in this paper is financially supported by China Light & Power (CLP) Holding Limited (Hong Kong) and The Hong Kong Polytechnic University. The authors would also like to

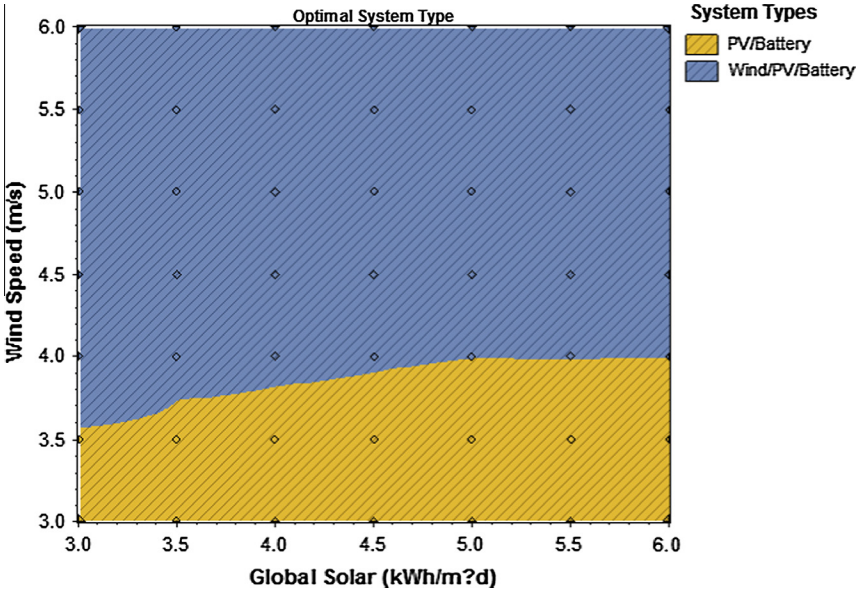

Fig. 16. Optimal system type against with solar radiation and wind speed.

thank Mr. C. C. Ngan and Mr. Raymond Ho from CLP for their valuable comments and suggestions on this work.

References

[1] Muneer T, Asif M, Kubie J. Generation and transmission prospects for solar electricity: UK and global markets. Energy Convers Manage 2003;44:35–52.
[2] WHO. The Energy Access Situation in Developing Countries: A Review Focusing on the Least Developed Countries and Sub-Saharan Africa. World Health Organization (WHO) and United Nations Development Programme (UNDP) (New York and Geneva), 2009.
[3] IEA. World Energy Outlook, 2nd ed. International Energy Agency Publications; 2006.
[4] Qoaider L, Steinbrecht D. Photovoltaic systems: a cost competitive option to supply energy to off-grid agricultural communities in arid regions. Appl Energy 2010;87:427–35.
[5] Ma T, Yang H, Lu L. Feasibility study and economic analysis of pumped hydro storage and battery storage for a renewable energy powered island. Energy Conversion and Management; 2014.
[6] Kaldellis JK, Zafirakis D, Stavropoulou V, Kaldelli E. Optimum wind- and photovoltaic-based stand-alone systems on the basis of life cycle energy analysis. Energy Policy 2012;50:345–57.
[7] Bajpai P, Dash V. Hybrid renewable energy systems for power generation in stand-alone applications: a review. Renew Sustain Energy Rev 2012;16:2926–39.
[8] Kaldellis JK, Kavadias KA, Koronakis PS. Comparing wind and photovoltaic stand-alone power systems used for the electrification of remote consumers. Renew Sustain Energy Rev 2007;11:57–77.
[9] Yang H, Wei Z, Chengzhi L. Optimal design and techno-economic analysis of a hybrid solar–wind power generation system. Appl Energy 2009;86:163–9.
[10] Kapsali M, Anagnostopoulos JS, Kaldellis JK. Wind powered pumped-hydro storage systems for remote islands: a complete sensitivity analysis based on economic perspectives. Appl Energy 2012;99:430–44.
[11] Zhao B, Zhang X, Li P, Wang K, Xue M, Wang C. Optimal sizing, operating strategy and operational experience of a stand-alone microgrid on Dongfushan Island. Appl Energy 2014;113:1656–66.
[12] Bernal-Agustín JL, Dufo-López R. Simulation and optimization of stand-alone hybrid renewable energy systems. Renew Sustain Energy Rev 2009;13:2111–8.
[13] Kaldellis JK, Zafirakis D. Optimum sizing of stand-alone wind-photovoltaic hybrid systems for representative wind and solar potential cases of the Greek territory. J Wind Eng Ind Aerodyn 2012;107–108:169–78.
[14] Yang H, Zhou W, Lu L, Fang Z. Optimal sizing method for stand-alone hybrid solar–wind system with LPSP technology by using genetic algorithm. Sol Energy 2008;82:354–67.
[15] Kaldellis JK, Zafirakis D, Kavadias K. Minimum cost solution of wind–photovoltaic based stand-alone power systems for remote consumers. Energy Policy 2012;42:105–17.
[16] Lujano-Rojas JM, Dufo-López R, Bernal-Agustín JL. Optimal sizing of small wind/battery systems considering the DC bus voltage stability effect on energy capture, wind speed variability, and load uncertainty. Appl Energy 2012;93:404–12.
[17] Chen H-C. Optimum capacity determination of stand-alone hybrid generation system considering cost and reliability. Appl Energy 2013;103:155–64.
[18] Connolly D, Lund H, Mathiesen BV, Leahy M. A review of computer tools for analysing the integration of renewable energy into various energy systems. Appl Energy 2010;87:1059–82.
[19] Luna-Rubio R, Trejo-Perea M, Vargas-Vázquez D, Ríos-Moreno GJ. Optimal sizing of renewable hybrids energy systems: a review of methodologies. Sol Energy 2012;86:1077–88.
[20] Lambert T, Gilman P, Lilienthal P. Micropower system modeling with homer. Integration of alternative sources of energy. John Wiley & Sons, Inc.; 2006. p. 379–418.
[21] Kaldellis JK, Gkikaki A, Kaldelli E, Kapsali M. Investigating the energy autonomy of very small non-interconnected islands: a case study: Agathonisi, Greece. Energy Sust Dev 2012;16:476–85.
[22] Khan MJ, Iqbal MT. Pre-feasibility study of stand-alone hybrid energy systems for applications in Newfoundland. Renew Energy 2005;30:835–54.
[23] Bekele G, Tadesse G. Feasibility study of small Hydro/PV/Wind hybrid system for off-grid rural electrification in Ethiopia. Applied Energy. 2012.
[24] Shaahid SM, Elhadidy MA. Economic analysis of hybrid photovoltaic–diesel–battery power systems for residential loads in hot regions—a step to clean future. Renew Sustain Energy Rev 2008;12:488–503.
[25] Ma T, Yang H, Lu L. Performance evaluation of a stand-alone photovoltaic system on an isolated island in Hong Kong. Appl Energy 2013;112:663–72.
[26] Yang H, Lu L, Zhou W. A novel optimization sizing model for hybrid solar–wind power generation system. Sol Energy 2007;81:76–84.
[27] Yang HX, Lu L, Burnett J. Weather data and probability analysis of hybrid photovoltaic–wind power generation systems in Hong Kong. Renew Energy 2003;28:1813–24.
[28] Muralikrishna M, Lakshminarayana V. Hybrid (solar and wind) energy systems for rural electrification. ARPN J Eng Appl Sci 2009(3).
[29] Zhou W, Lou C, Li Z, Lu L, Yang H. Current status of research on optimum sizing of stand-alone hybrid solar–wind power generation systems. Appl Energy 2010;87:380–9.
[30] Lau KY, Yousof MFM, Arshad SNM, Anwari M, Yatim AHM. Performance analysis of hybrid photovoltaic/diesel energy system under Malaysian conditions. Energy 2010;35:3245–55.
[31] Stand-Alone Photovoltaic Systems: A Handbook of Recommended Design Practices, SAND87-7023. Albuquerque, NM: Photovoltaic Design Assistance Center, Sandia National Laboratories; March, 1995.
[32] Manwell JF, McGowan JG. Lead acid battery storage model for hybrid energy systems. Sol Energy 1993;50:399–405.
[33] Lambert T, Gilman P, Lilienthal P. Micropower system modeling with homer, 2006. <wwwmistayaca/software/docs/MicropowerSystemModelingWithHOMERpdf>.
[34] Gota D-I, Lund H, Miclea L. A Romanian energy system model and a nuclear reduction strategy. Energy 2011;36:6413–9.
[35] Østergaard PA, Lund H. A renewable energy system in Frederikshavn using low-temperature geothermal energy for district heating. Appl Energy 2011;88:479–87.
[36] Elliston B, Diesendorf M, MacGill I. Simulations of scenarios with 100% renewable electricity in the Australian National Electricity Market. Energy Policy 2012;45:606–13.